Regional emission metrics for short-lived climate forcers from multiple models

Aamaas, B., Berntsen, T. K., Fuglestvedt, J. S., Shine, K. P. and Bellouin, N. (2016) Regional emission metrics for short-lived climate forcers from multiple models. Atmospheric Chemistry and Physics, 16 (11). pp. 7451-7468. ISSN 1680-7316 doi: https://doi.org/10.5194/acp-16-7451-2016 Available at http://centaur.reading.ac.uk/65885/

Published version at: http://dx.doi.org/10.5194/acp-16-7451-2016

To link to this article DOI: http://dx.doi.org/10.5194/acp-16-7451-2016

Publisher: Copernicus Publications

Atmos. Chem. Phys., 16, 7451–7468, 2016
www.atmos-chem-phys.net/16/7451/2016/
doi:10.5194/acp-16-7451-2016

Atmospheric Chemistry and Physics Open Access EGU

Regional emission metrics for short-lived climate forcers from multiple models

Borgar Aamaas[1], Terje K. Berntsen[2,3], Jan S. Fuglestvedt[1], Keith P. Shine[3], and Nicolas Bellouin[3]

[1]Center for International Climate and Environmental Research – Oslo (CICERO), PB 1129 Blindern, 0318 Oslo, Norway
[2]Department of Geosciences, University of Oslo, Oslo, Norway
[3]Department of Meteorology, University of Reading, Reading, UK

Correspondence to: Borgar Aamaas (borgar.aamaas@cicero.oslo.no)

Received: 8 July 2015 – Published in Atmos. Chem. Phys. Discuss.: 25 September 2015
Revised: 1 June 2016 – Accepted: 2 June 2016 – Published: 15 June 2016

Abstract. For short-lived climate forcers (SLCFs), the impact of emissions depends on where and when the emissions take place. Comprehensive new calculations of various emission metrics for SLCFs are presented based on radiative forcing (RF) values calculated in four different (chemical-transport or coupled chemistry–climate) models. We distinguish between emissions during summer (May–October) and winter (November–April) for emissions in Europe and East Asia, as well as from the global shipping sector and global emissions. The species included in this study are aerosols and aerosol precursors (BC, OC, SO_2, NH_3), as well as ozone precursors (NO_x, CO, VOCs), which also influence aerosols to a lesser degree. Emission metrics for global climate responses of these emissions, as well as for CH_4, have been calculated using global warming potential (GWP) and global temperature change potential (GTP), based on dedicated RF simulations by four global models. The emission metrics include indirect cloud effects of aerosols and the semi-direct forcing for BC. In addition to the standard emission metrics for pulse and sustained emissions, we have also calculated a new emission metric designed for an emission profile consisting of a ramping period of 15 years followed by sustained emissions, which is more appropriate for a gradual implementation of mitigation policies.

For the aerosols, the emission metric values are larger in magnitude for emissions in Europe than East Asia and for summer than winter. A variation is also observed for the ozone precursors, with largest values for emissions in East Asia and winter for CO and in Europe and summer for VOCs. In general, the variations between the emission metrics derived from different models are larger than the variations between regions and seasons, but the regional and seasonal variations for the best estimate also hold for most of the models individually. Further, the estimated climate impact of an illustrative mitigation policy package is robust even when accounting for the fact that the magnitude of emission metrics for different species in a given model is correlated. For the ramping emission metrics, the values are generally larger than for pulse or sustained emissions, which holds for all SLCFs. For SLCFs mitigation policies, the dependency of metric values on the region and season of emission should be considered.

1 Introduction

Climate is impacted by various emitted gases and particles with a range of radiative efficiencies, lifetimes, and climate efficacies (e.g., Myhre et al., 2013). Emissions of CO_2, N_2O, and some of the other gases included in the Kyoto Protocol are defined as long-lived greenhouse gases (LLGHGs). In addition, emissions of black carbon (BC), organic carbon (OC), SO_2, NH_3, NO_x, CO, and volatile organic compounds (VOCs) cause changes in atmospheric levels of short-lived climate forcers (SLCFs), such as ozone and aerosols (BC, OC, sulfate, and nitrate). As CH_4 has an atmospheric perturbation lifetime of about 10 years, this gas is generally as well mixed as the LLGHGs but is often categorized together with the SLCFs since its lifetime is shorter than a realistic timescale for stabilizing anthropogenic influence on climate. There has recently been increased interest by policymakers to mitigate these SLCFs, for instance as advocated by the

Climate and Clean Air Coalition (CCAC), motivated by co-benefits to climate and air quality (e.g., Schmale et al., 2014). Smith and Mizrahi (2013) find that the climate benefits for the next few decades of reducing SLCFs today are comparable to a climate policy on LLGHGs. However, Myhre et al. (2011) point out that reducing emissions of SLCFs today might potentially result in a delay in CO_2 mitigation, which may give unwanted long-term consequences (Pierrehumbert, 2014). Studies show that climate change in the long term is mainly governed by CO_2 emissions; however, mitigation of SLCFs may temporarily decrease the rate of warming (Shoemaker et al., 2013; Bowerman et al., 2013). Rogelj et al. (2014) argue that quantifying the climate impact of actual mitigation policies targeted on SLCFs is difficult, as the sources are common for a range of SLCFs and LLGHGs; thus, these linkages should be considered. Recently Allen et al. (2016) showed that the global warming potential with a time horizon of 100 years (GWP(100)) effectively measures the relative impact of both cumulative species and SLCFs on realized warming 20–40 years after the time of emission. They also showed that GWP(100) can be used to approximately equate a one-off pulse emission of a cumulative pollutant and an indefinitely sustained change in the rate of emission of an SLCFs, which introduces a new application when SLCFs, CO_2, and other LLGHGs are compared.

The impact of emissions of different SLCFs may be measured with the use of emission metrics which quantify an idealized climate impact per unit mass of emissions of a given species. Various applications exist (Fuglestvedt et al., 2003; Tanaka et al., 2010; Aamaas et al., 2013), the main ones are to (1) provide an "exchange rate" between different emitted species used in mitigation policies, (2) compare different activities and technologies that emit a range of species over time such as in life cycle assessment (LCA), and (3) compare in a simplified manner the climate responses of various emissions to gain and communicate scientific understanding. The most common emission metrics are time integrated radiative forcing (absolute global warming potential, AGWP) (IPCC, 1990) and temperature perturbation (absolute global temperature change potential, AGTP) (Shine et al., 2005; Shine et al., 2007), which, when normalized to CO_2, become GWP and GTP, respectively. Physically based metrics evaluate the idealized climate impact (integrated global mean RF for GWP or global mean temperature change for the GTP) over a certain time period (for the GWP) or at a given time after the emissions (for the GTP). This time period is called the time horizon and this choice is inevitably influenced by value judgments. Here we present metric values for a range of time horizons. Among the value choices are, for instance, looking at either temperature or forcing and what time horizon to pick (Fuglestvedt et al., 2003; Tol et al., 2012; Myhre et al., 2013). The Kyoto Protocol used GWP with a time horizon of 100 years.

Emissions metrics have normally been calculated for global emissions. However, for SLCFs, due to their short lifetimes compared to large-scale atmospheric mixing times, and because the chemistry and radiative effects on climate depends on the regional physical conditions, even the global mean radiative forcing depends on the region of emissions (Fuglestvedt et al., 1999; Wild et al., 2001; e.g., Berntsen et al., 2005; Naik et al., 2005). Then, the emission metric values will vary for different emission locations (Fuglestvedt et al., 2010). In addition, distinct patterns in the temperature response appear from all forcings (Boer and Yu, 2003; Shindell et al., 2010). A growing literature investigates how the weights of the emission metrics change as emissions from different regions of the world are considered. Collins et al. (2013) assessed variations in emission metrics for four different regions (East Asia, Europe, North America, and South Asia) for aerosols and ozone precursors, based on radiative forcings from consistent multimodel experiments from the Hemispheric Transport of Air Pollution (HTAP) experiments given by Yu et al. (2013) and Fry et al. (2012). Collins et al. (2010) also investigated how emission metric values differ between regions, including vegetation responses. Bond et al. (2011) quantified differences in RFs for BC and OC emissions from different locations and types of emissions.

For SLCFs, the impact also depends upon the season of emissions. As the chemistry and radiative effects vary between summer and winter, the RF per unit emissions will differ between the seasons. An additional factor is that the magnitude of emissions fluctuates between the seasons, which can also be the case for LLGHGs. For example, emissions of certain species from wood burning for domestic heating will be much larger in winter than summer (Streets et al., 2003).

Bellouin et al. (2016) detail a comprehensive set of dedicated RF calculations with four models (ECHAM6-HAMMOZ, HadGEM3-GLOMAP, NorESM, and OsloCTM2) for emission perturbations in different regions (Europe, East Asia, shipping, and global) and seasons (Northern Hemisphere (NH) summer (May–October) and winter (November–April)) for various SLCFs or their precursors (BC, OC, SO_2, NH_3, NO_x, CO, and VOCs) and for global annual emissions of CH_4. Here, we present separate emission metric values for emissions during NH summer and winter emissions. In this study, we use the RF results from Bellouin et al. (2016) to calculate emission metrics for the different regions and seasons. We produce emission metrics for standard pulse emissions as well as for an emission profile consisting of a ramped period of 15 years followed by a sustained case, which can illustrate a gradual implementation of technology standards. As the study is based on several models running the same experiments, these data allow us to investigate the robustness in our findings. We analyze the robustness for individual species, as well as for hypothetical policy mitigation packages. Finally, we discuss how the emission metrics presented here can be used in mitigation policies.

2 Material and methods

2.1 Radiative forcing

An overview of the four different coupled chemistry–climate models or chemical-transport models presented by Bellouin et al. (2016), their resolution and species investigated (SO_2, BC, OC, NH_3, NO_x, CO, VOCs, and CH_4) is given in Table 1. Not all models have calculated RF for all species. While all four models give RFs for BC, OC, and SO_2, only the OsloCTM2 calculated RF for NH_3. Three models (OsloCTM2, HadGEM3, NorESM) have calculated RFs for the ozone precursors and CH_4.

The calculations are based on different processes that affect RF (see Bellouin et al., 2016). For aerosols and aerosol precursors, three of the four models calculate the aerosol direct and first indirect (cloud-albedo) effect, with ECHAM6 only diagnosing direct RF. For BC, OsloCTM2 estimated in addition the RF from BC deposition on the snow and semi-direct effect. Only a few previous studies, such as Bond et al. (2013), have included the semi-direct effect in emission metrics. For the ozone precursors and CH_4, the total RF consists of the aerosol direct and first indirect effects, short-lived ozone effect, methane effect, and methane-induced ozone effect. Only OsloCTM2 includes nitrate aerosols, but nitrate aerosol RF has been used to complement the estimates by other models.

The best estimate of a species' RF is given as the sum of all the processes, in which the average across the models is used for each process. ECHAM6 is not included in the best estimate for BC, OC, and SO_2, since this model does not diagnose the first indirect effect. The best estimate is based on only the OsloCTM2 model for BC deposition on snow and BC semi-direct effect, while the best estimates are based on three models for all other processes (aerosol effects, short-lived ozone, methane, and methane-induced ozone).

For the high and low estimate, we sum the highest and lowest values, respectively, for each individual process.

These global-mean RFs of various species were calculated for emissions in different regions. The three regions, following tier 1 HTAP regions, are Europe (western and eastern Europe up to 66° N, including Turkey), East Asia (China, Korea, and Japan), and the global shipping sector. RF values are also available from remaining land areas outside of Europe and East Asia; results for this case are presented in the Supplement (Sect. S1). Values for global emissions were also utilized. Emissions from shipping are not included in the global estimates since only OsloCTM2 and NorESM include detailed estimates for the shipping sector. All estimates are given for NH summer and NH winter. As emissions globally and from the shipping sector occur in both hemispheres, the two seasons are a mix of summer and winter conditions. For these two cases, we refer to NH winter and NH summer.

2.2 Emission metrics

In this study, we use the emission metrics GWP and GTP with varying time horizons. In all perturbations, RF is annually and globally averaged; thus, the responses are also annually averaged. AGWP for species i at time horizon H is defined as

$$\mathrm{AGWP}_i\,(H) = \int_0^H \mathrm{RF}_i\,(t)\,\mathrm{d}t, \tag{1}$$

where RF is the time-varying radiative forcing following a unit mass pulse emission at time zero. The calculations of the RFs build on the framework previously shown for short-lived ozone depletion gases for the metric the ozone depletion potential (Olsen et al., 2000; Bridgeman et al., 2000; Wuebbles et al., 2001). This work led to the mathematical relationship between the steady-state impacts from sustained emissions, the pulse response function, and the steady-state lifetime (Prather, 2002), which we follow in our RF calculations. For aerosols, the radiative forcing values ($\mathrm{RF_{ss}}$) ($\mathrm{W\,m^{-2}(kg\,yr^{-1})^{-1}}$) calculated by Bellouin et al. (2016) are based on assuming that the emissions are sustained for a year and hence the concentrations are close to equilibrium values because of their short steady-state lifetimes. These $\mathrm{RF_{ss}}$ values have been converted into RF values ($\mathrm{W\,m^{-2}\,kg^{-1}}$) for an instantaneous emission for BC, OC, SO_2, and NH_3 by the formula (Aamaas et al., 2013)

$$\mathrm{RF} \approx \frac{\mathrm{RF_{ss}}}{\tau}, \tag{2}$$

where τ is the perturbation lifetime (years) of the aerosol species. This conversion is only applicable when the adjustment time of the species is significantly less than 1 year. The adjustment time can be dependent on different processes with different timescales, such as wet and dry deposition. The perturbation lifetimes are model specific and given in Bellouin et al. (2016).

The AGTP is given as

$$\mathrm{AGTP}_i\,(H) = \int_0^H \mathrm{RF}_i\,(t)\,\mathrm{IRF}_T\,(H-t)\,\mathrm{d}t, \tag{3}$$

where $\mathrm{IRF}_T\,(H-t)$ is the impulse response function for temperature at time H to a unit radiative forcing at time t. The equations for the AGTP calculations for aerosols and ozone pre-cursors are given in Aamaas et al. (2013). These emissions metrics (AGWP, AGTP) are given in absolute forms. They can be normalized to the corresponding effect of CO_2, where M is GWP or GTP, given as

$$M_i\,(t) = \frac{\mathrm{AM}_i\,(t)}{\mathrm{AM}_{\mathrm{CO_2}}\,(t)}. \tag{4}$$

To calculate the time-varying RF for a pulse emission of CO_2 an impulse response function ($\mathrm{IRF_C}$) for CO_2 is

Table 1. General circulation models (GCMs) and chemical transport models (CTMs) used to calculate radiative forcing in this study. Resolution shows the horizontal resolution and the number of vertical layers. Radiative forcing has been calculated for emissions of these gases and particles by Bellouin et al. (2016).

Model	Type	Resolution	BC	OC	SO_2	NH_3	NO_x	CO	VOCs	CH_4	References
ECHAM6-HAMMOZ	GCM	1.8° × 1.8° L31	X	X	X						Stevens et al. (2013)
HadGEM3-GLOMAP	GCM	1.8° × 1.2° L38	X	X	X		X	X	X	X	Hewitt et al. (2011)
NorESM	GCM	1.9° × 2.5° L26	X	X	X		X	X	X	X	Bentsen et al. (2013), Iversen et al. (2013)
OsloCTM2	CTM	2.8° × 2.8° L60	X	X	X	X	X	X	X	X	Søvde et al. (2008), Myhre et al. (2009)

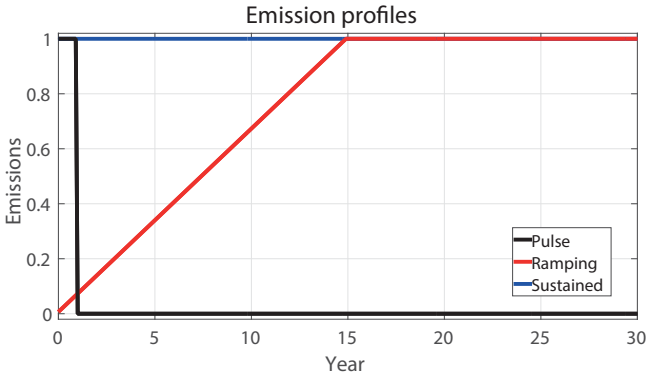

Figure 1. Pulse, sustained, and ramping emission profiles. The ramping period can vary.

needed. Here we use the IRF_C based on the Bern Carbon Cycle Model (Joos et al., 2013) as reported in Myhre et al. (2013). The IRF_T is here treated independently of the emitted species and based on simulations with the Hadley Centre CM3 climate model (Boucher and Reddy, 2008). These parameterizations have uncertainties, and Olivié and Peters (2013) studied the effective of different IRF_T from different atmosphere–ocean general circulation models and found that the uncertainty is the largest for the most short-lived SLCFs.

Emission metrics for pulse emissions are in principle the most useful metrics, even though emissions follow a given temporal profile. A pulse can be seen as an instantaneous emission, or constant emission during a short period ($\ll H$), followed by no emissions. In the real world, implementing mitigation can be a gradual process where emissions are gradually reduced over some period, followed by a sustained level of emission reduction. This reflects regulations or technical improvements that are phased in over a given period and then sustained indefinitely. Such an emission profile, or mitigation profile, can be called a "ramping". These different types of emission profiles are shown in Fig. 1. For ramping or any other emissions scenarios, the emission metric can be calculated by a convolution. A temperature response is calculated as

$$\Delta T_i(t) = \int_0^t E_i\left(t'\right) \mathrm{AGTP}_i\left(t - t'\right) \mathrm{d}t'. \quad (5)$$

E is the emission scenario and AGTP gives the temporal temperature perturbation for a unit of emissions. The absolute metrics for compound i for the ramping scenarios ($\mathrm{AM}_i^{\mathrm{R}}$) are calculated according to

$$\mathrm{AM}_i^{\mathrm{R}}(H) = \sum_{t_e=0}^{H} E_i(t_e) \cdot \mathrm{AM}_i^{\mathrm{p}}(H - t_e), \quad (6)$$

where $\mathrm{AM}_i^{\mathrm{p}}(H)$ is the corresponding absolute pulse metric (e.g., AGWP or AGTP) for time horizon H, and $E(t_e)$ is the emission at time t_e. The integral in Eq. (5) is the general notation, while we apply this in our calculations with the sum in Eq. (6). Note that the sustained case is a special case where $E(t) = E_s$ for all t. For a ramping period of mitigation of TH years (where TH stands for time horizon), emissions in year t in the first TH years are $E(t_e) = \frac{t_e \cdot E_s}{\mathrm{TH}}$ and after that E_s. We show results only for a ramping period of TH = 15 years, but we have also investigated other implementation rates. The total response for a scenario is found by multiplying Eq. (6) with the total emission change. Note that since emission metric values for SLCFs increase with decreasing time horizon (because they are short-lived), their "ramping" emission metrics values are significantly higher than the standard pulse-based values.

Emission metrics normalized to the corresponding absolute emission metric for ramping emissions of CO_2 ($M_i^{\mathrm{R}}(H)$) are calculated by

$$M_i^{\mathrm{R}}(H) = \frac{\mathrm{AM}_i^{\mathrm{R}}(H)}{\mathrm{AM}_{\mathrm{CO_2}}^{\mathrm{R}}(H)}. \quad (7)$$

Note that since the pulse metrics are given by region and season, so are the ramping metrics ($M_i^{\mathrm{R}}(H)$).

For policymakers to apply this concept to compare different (n) sets of mitigation options (all following the same ramping profiles over time, but with different mix of species, regions, and seasons), the net impacts ($I_{\mathrm{n}}(H)$)(i.e., AGWP or AGTP) for all options must be calculated according to

$$I_{\mathrm{n}}(H) = \sum_j \sum_i \Delta E_i(j) \cdot M_i^{\mathrm{R}}(H). \quad (8)$$

Here $\Delta E_i(j)$ denotes the total mitigation (e.g., at the end of the ramping period) of component i emitted in region j.

3 Results

3.1 Emission metric values

3.1.1 Best estimates

First, we present the best estimate of emission metric values for pulse emissions; see Table 2 for GTP(20) values. Additional values for GWP and for other selected time horizons are given in Table S1 in the Supplement. Due to space constraints, we can only present values for a few time horizons. The choice of emission metric and time horizon depends on the application, and a range of different justified choices are possible (e.g., Aamaas et al., 2013). If the focus is on temperature change in the next few decades, GTP(20) is appropriate. In Fig. 2, GTP(20) values are given for the different species, decomposed by a range of processes. Figure 3 presents results for GWP(100) for the ozone precursors. We first focus on a few selected time horizons, but Sect. 3.1.5 shows how emission metrics evolve for a range of time horizons.

The uncertainties in Figs. 2 and 3 are given as the range across all contributing models. The uncertainty is in general larger than the variation between different regions and seasons. Thus, when including the uncertainty, it is less clear which region and season give the largest and smallest emission metric values. However, we will show in Sects. 3.1.3 and 3.1.4 that the best estimate is more robust than the uncertainty bars indicate.

The emission metric values for the shipping sector are based on only two models (OsloCTM2 and NorESM). We do not provide uncertainty ranges for shipping due to the low numbers of models. Further, the robustness of these values presented is lower than for the other regions for the same reason.

We find distinct differences between regions and seasons for all species. For the aerosols BC, OC, and SO_2, the magnitude of the total GTP(20) values is higher for emissions during summer than winter and larger for Europe than for East Asia. However, the emission metric value for winter emissions of BC is only slightly higher for Europe than for East Asia. The higher emission metric values for Europe than for East Asia is likely caused by a more polluted baseline in East Asia, which leads to a saturation for some of the interactions. Collins et al. (2013) also estimated higher values for Europe than East Asia, while Fuglestvedt et al. (2010) based on earlier calculations in the literature gave partly conflicting results. As a significant share of the emissions from the shipping sector, as well for global emissions, are occurring in the Northern Hemisphere, the seasonal variation is similar for these two categories except for BC for shipping. Seasonal variations are mainly driven by aerosol RF, which is mainly located in the shortwave spectrum. Greater sunlight duration in local summer yields stronger RFs (Bellouin et al., 2016). Seasonal differences in atmospheric lifetimes, caused by seasonality in precipitation, will also contribute.

For BC, the elevated aerosol effect in summer is partially canceled out by a cooling effect by the semi-direct effect (see Fig. 2). The semi-direct effect is due to the absorption of solar radiation of particles, which affects the atmospheric static stability, and impacts on clouds. The impact of BC deposition on snow is largest for emissions during winter and larger for Europe than East Asia. The BC surface albedo effect is governed by the extent of snow- and ice-covered surface area but also depends on the availability of solar radiation where the BC is deposited. For Europe, the snow effect is 54 % of the direct effect in winter and 2.61 % in summer, while the corresponding percentages are 22 and 1.1 % for East Asia. The shares are similar for the shipping and global, with lowest shares for global emissions. As explained by Bellouin et al. (2016), this is due to atmospheric transport: according to the models, European emissions of BC are preferentially transported to the Arctic, where they modify the albedo of snow. Seasonality is driven by snow cover, which is larger in winter and early spring. In Europe, the semi-direct effect is -38 % of the direct effect in summer and -9.5 % in winter, while it is -42 and 4.4 %, respectively, for East Asia. As the other regions are a mix of summer and winter because both hemispheres are included, the semi-direct effect is smeared out over the two seasons, but largest in absolute value for NH summer. For NH_3, the GTP(20) value is larger for Europe than East Asia in summer but not for winter, as explained by Bellouin et al. (2016). Ammonium nitrate aerosol formation is strongly dependent on relative humidity and temperature, and competes for ammonium with ammonium sulfate aerosols, which has larger concentrations in local summer (Bellouin et al., 2011). Those complex interactions may explain different seasonalities in different regions, and will contribute to model diversity.

For the ozone precursors, the variability between regions and seasons is smallest for CO. For CO, GTP(20) values are higher for winter than summer. Due to the longer lifetime of CO during winter, a large fraction of the CO emitted during winter will undergo long-range transport and will be oxidized in relatively clean low-NO_x environments. There CO-oxidation will reduce OH and thus increase the methane lifetime. As can be seen in Fig. 2, it is the indirect methane effect that leads to higher metric values for wintertime emissions. Furthermore, GTP(20) values of CO are slightly larger for East Asia than Europe. For VOCs, the seasonal variability is opposite with highest GTP(20) values for summer. Further, GTP(20) values are higher for Europe than East Asia. The overall picture is a bit more complex for NO_x. The seasonal difference is very small for GTP(20) values in East Asia. However, for Europe, the GTP(20) value is more negative for summer and less negative for winter. Shipping has the largest GTP(20) values in magnitude for all ozone precursors, especially the large methane effect, driven by the relatively clean atmospheric conditions around the emission locations. The models may overestimate the ozone production of NO_x emissions from shipping, as they do not represent

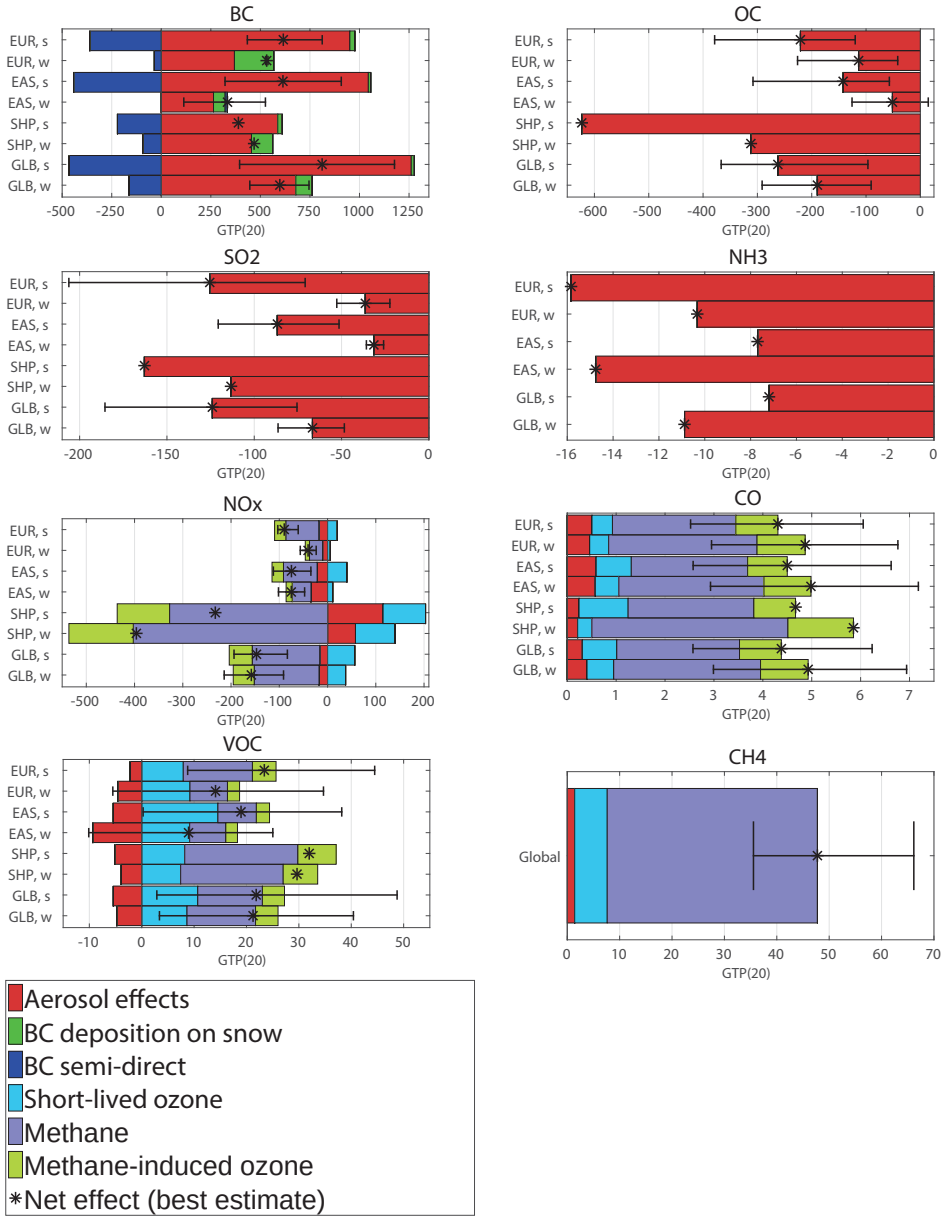

Figure 2. GTP(20) values for the species, for all regions and seasons, decomposed by processes. The regions included are Europe (EUR), East Asia (EAS), shipping (SHP), and global (GLB), all for both NH summer (s), May–October, and NH winter (w), November–April. How the best estimate of the net effect is calculated is given in Sect. 2.1. The uncertainty bars show the range across models, which is not given for shipping as the best estimate is based on only two models for that sector. For CH_4 emissions, the ozone effect is formally classified as short-lived ozone, but the perturbation timescale is the same as for the methane-induced ozone effect.

ship plumes, but assume instantaneous dilution of emissions in the grid boxes (Paoli et al., 2011). Holmes et al. (2014) obtained a 40 % decrease in ship NO_x RF when they improved their representation of ship plume chemistry. It is therefore possible that the RF for NO_x is overestimated by 50 % or more. Collins et al. (2013) observed the same annual pattern for Europe and East Asia as we do. One notable feature for NO_x is that the aerosol effect is negative for all cases except for shipping, mainly because the values for shipping are based on two models and the other values are based on three models. The positive value for shipping is the average of two models with opposing signs; thus, there is significant uncertainty in the best estimate. This model disagreement for NO_x is discussed in detail by Bellouin et al. (2016).

For aerosols emissions and the major aerosols precursors, the relative ratios between the different regions and seasons are constant while varying the emission metric and time horizon applied. On the other hand, the relative ratios between

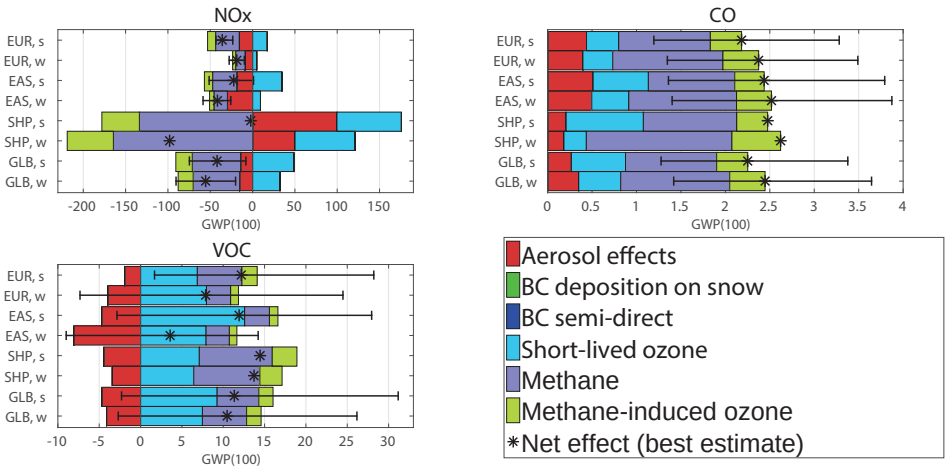

Figure 3. GWP(100) values for the ozone precursors, for all regions and seasons, decomposed by processes. The regions included are Europe (EUR), East Asia (EAS), shipping (SHP), and global (GLB), all for both NH summer (s), May–October, and NH winter (w), November–April. How the best estimate of the net effect is calculated is given in Sect. 2.1. The uncertainty bars show the range across models, which is not given for shipping as the best estimate is based on only two models for that sector.

Table 2. The best estimate given for GTP(20) values. The component of each species which the mass emission refers to is shown in brackets. The regions are Europe (EUR), East Asia (EAS), shipping (SHP), and global (GLB), for emissions occurring in NH summer (s), May–October, and NH winter (w), November–April.

GTP(20)	BC [C]	OC [C]	SO_2 [SO_2]	NH_3 [NH_3]	NO_x [N]	CO [CO]	VOCs [C]	CH_4 [CH_4]
EUR, s	620	−220	−130	−16	−90	4.3	23	48
EUR, w	530	−110	−36	−10	−40	4.9	14	48
EAS, s	610	−140	−87	−7.7	−75	4.5	19	48
EAS, w	330	−50	−31	−15	−75	5.0	8.9	48
SHP, NH s	390	−620	−160	NA	−230	4.7	32	48
SHP, NH w	470	−310	−110	NA	−400	5.9	30	48
GLB, NH s	810	−260	−120	−7.2	−150	4.4	22	48
GLB, NH w	600	−190	−67	−11	−160	4.9	21	48

different emission metric values for the ozone precursors differ with varying emission metrics and time horizons. The ratios for the aerosols are fixed since the aerosols have little effect on perturbations of atmospheric composition and components with long adjustment times. By contrast, the ozone precursors affect processes with longer time constants. By causing a change in OH levels, methane with an adjustment time of about 10 years is perturbed. Hence, we also show GWP(100) values for the ozone precursors (Fig. 3), while similar figures for the other species are provided in the Supplement (Fig. S1). For the ozone precursors, the aerosol direct and indirect effect and the short-lived ozone effect are given relatively more weight for GWP(100) than GTP(20) than the methane effect and methane-induced ozone effect, since GWP integrates the RF up to the time horizon, while GTP is an end-point indicator. As the time horizon increases, the relative contribution from methane and methane-induced ozone increases and the contribution from aerosols and short-lived ozone decreases. The overall picture presented here for GTP(20) and GWP(100) is mostly similar. However, for NO_x, no significant seasonal difference was observed in GTP(20) values for East Asia, while the value in winter is almost twice as negative as the summer values for GWP(100). For shipping emissions in NH summer, the emission metric value changes from clearly negative for GTP(20) to almost zero for GWP(100).

We provide only one global emission metric value for CH_4, as CH_4 emissions are relatively well mixed in the atmosphere and expected differences due to regionality and seasonality are small (Bellouin et al., 2016). The aerosol effect is weakly positive, while the models give a wide range from weakly negative to strongly positive, as discussed in Bellouin et al. (2016).

3.1.2 Comparison with the literature

As already noted, the variations with respect to regional emissions for emission metric values are in line with Collins et al. (2013). Fuglestvedt et al. (2010) also presented emis-

sion metrics with respect to regional emissions based on earlier calculations in the literature, but with some conflicting results between available studies. Due to this spread, our findings are partly in line with Fuglestvedt et al. (2010). In general, the specific emission metric values are also comparable with Collins et al. (2013). However, a complete comparison is not possible as we have included the effect of aerosols for the ozone precursors and the semi-direct and deposition on snow effect for BC. The findings are also generally similar to previous estimates for emission metrics of global emissions (e.g., Fuglestvedt et al., 2010), with some discrepancies we will discuss here. A comparison of modeled GWP and GTP values with a selection from the literature for some selected time horizons is given in Table S1.

For BC, Bond et al. (2013, 2011) presented about 20–40 % higher emission metric values (GTP and GWP), while other studies (Fuglestvedt et al., 2010; Collins et al., 2013) are in line with or up to 40 % lower than this study and Hodnebrog et al. (2014) give significant lower values. As discussed in Hodnebrog et al. (2014), the atmospheric lifetime of BC may be shorter and the BC emissions may be larger than previously thought (e.g., Fuglestvedt et al., 2010), leading to emission metric values almost halved compared to previous estimates (−44 % for the example given in Hodnebrog et al., 2014). The OC values in our study are more than 200 % higher in magnitude than the literature, driven by the high values in one of the models (NorESM). The OC values from NorESM are driven by a strong indirect effect. When this indirect effect is excluded, the NorESM value is similar to the others as well as the literature. For SO_2, the emission metric values for the winter season are similar to or up to 60 % stronger than the literature, while they are more than doubled for summer. As for OC, the more negative emission metric values for SO_2 are driven by the inclusion of the indirect effect. The one study (Shindell et al., 2009) we found on NH_3 gave emission metric values that are about double that of our annual average. The literature shows a wide range in the emission metric values for NO_x depending on the source and region. Our estimates are within this range but, on the more negative side within the range, about 80 % stronger than the values used for land-based emissions in Myhre et al. (2013). The emission metric values for CO are roughly 0–30 % higher than in the literature, partly driven by the additional positive impact of including the aerosol effect. For VOCs, the emission metric values are roughly double that or more than those found in the literature, even with a negative contribution from the aerosol effect (Bellouin et al., 2016). The emission metric values for CH_4 are mostly lower than those in Myhre et al. (2013) (29 and 19 % lower for GTP(20) and GWP(100), respectively), mainly due to a shorter methane atmospheric lifetime, as well as a smaller contribution from the indirect effect on ozone.

3.1.3 Robustness for individual species

The differences in the emission metric values between the emission regions and seasons of emissions seen for the best estimate holds generally in each model, which strengthens our confidence in the modeled variations between regions and seasons. For emissions of aerosols and their precursors, the magnitude of GTP(20) values is higher in summer than winter in 86 % of the model cases. The consistency between the individual models and our best estimate based on the models is 100 % for SO_2. The metric values for European emissions are larger in magnitude for most cases than East Asia. In summer, this is true for 92 % of the cases and 50 % in winter in addition to 33 % that are marginally the opposite. Yu et al. (2013) also observed that the regional dependency in RF was robust for a number of models with the same regional pattern as in our study.

For the ozone precursors, the variation in GTP(20) values observed for the best estimate also holds for most of the models. For both regional and seasonal variability, 83 % of the model cases agree with the best estimate. For CO, all cases agree that the GTP(20) values are larger for East Asian emissions than European emissions and for winter than summer, even though the relative differences in GTP(20) values between Europe and East Asia in summer and winter are relatively small. The difference may occur since the East Asia region is located closer to the Equator. The findings for NO_x and VOCs are also relatively robust, where the model cases agree 75 % for NO_x and 83 % for VOCs. The same tendencies in the regional pattern were also found by Collins et al. (2013).

3.1.4 Robustness in total climate impact

Emission metrics are used to quantify the climate impacts of different sets of emission changes following either mitigation policies or changes caused by some other mechanisms (e.g., technological development). However, the uncertainties given by the model ranges for individual regions, seasons, and species shown in Figs. 2 and 3 do not provide a good indication for the robustness of the *total* impacts estimated by the emission metrics, because there might be significant correlations between species. By robustness here, we mean how uncertain is the total climate impact of a given set of emission changes (changes of multiple species, seasons and regions) and related to this how robust would a ranking (in terms of net climate impact) of possible mitigation measures be, given the individual uncertainties shown in Figs. 2 and 3.

Models with more efficient vertical transport and/or slow removal of aerosols by wet scavenging will tend to give longer lifetimes for the aerosols and thus stronger RF per unit emission for all aerosol species, and thus emission metric values for the individual species and seasons would be correlated. This means that the ranking of measures and the

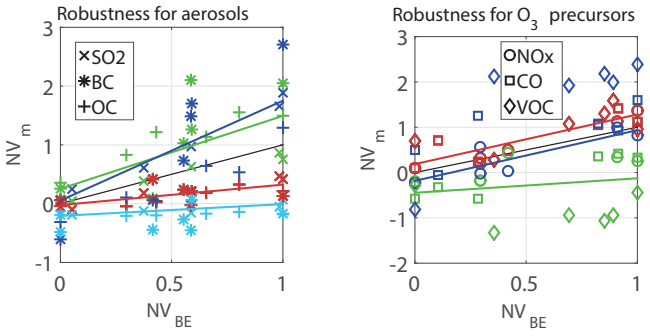

Figure 4. Scatter plot of the normalized variability of the model estimates (NV_m) versus NV_{BE} for the best estimate. Colors of the symbols indicate individual models (red: OsloCTM2; green: NorESM; blue: HadGEM3; and light blue: ECHAM6) and the shape of the symbol indicate individual species. Left panel: aerosols and aerosol precursors (BC, OC, and SO_2). Right panel: ozone precursors (NO_x, CO, and VOCs). The black line is the one-to-one line. The estimates use the GTP(20) emission metric.

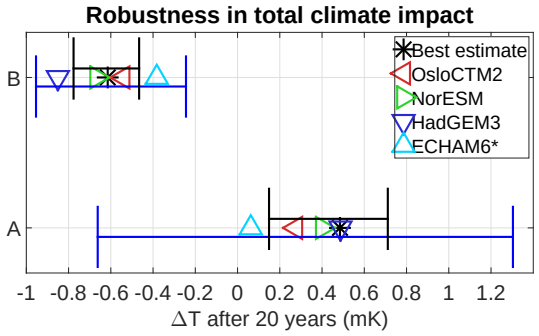

Figure 5. Emission metric-based estimate of change in global mean temperature by 10 % reduction in emissions of all SLCFs based on 2008 global emissions with positive best estimate AGTP(20) values (BC, CO, and VOCs, labeled B), and 10 % global reduction in all SLCFs (also including OC, SO_2, and NO_x, labeled A). Colored symbols use sets of emission metrics from individual models. The blue bar is given based on summing contributions using all maxima and minima in Fig. 2. The black bar is the uncertainty assuming the metric estimates are all independent.

net impact of measures that lead to reduction in emissions of co-emitted species that cause a cooling effect could be more robust. Similar effects can be expected across ozone precursors due to non-linear chemistry effects and removal efficiencies; for instance, such correlations across models were observed for the climate effect of NO_x emissions from aviation by Holmes et al. (2011). To investigate this we first focus on the correlation. To put all species on a common scale we calculate the normalized variability (across species, regions, and seasons) for the best estimate (NV_{BE}) and for the individual model estimates (NV_m):

$$\mathrm{NV_{BE}}\,(r,s,i) = \frac{M_{\mathrm{BE}}\,(r,s,i) - M_{\mathrm{BE,min}}(i)}{M_{\mathrm{BE,max}}\,(i) - M_{\mathrm{BE,min}}\,(i)}, \tag{9}$$

$$\mathrm{NV_m}\,(r,s,i) = \frac{M_{\mathrm{m}}\,(r,s,i) - M_{\mathrm{BE,min}}(i)}{M_{\mathrm{BE,max}}\,(i) - M_{\mathrm{BE,min}}\,(i)}. \tag{10}$$

$M_{\mathrm{BE}}(r,s,i)$ denotes the best estimate for the emission metric value for species i, region r, and season s, while $M_{\mathrm{m}}(r,s,i)$ denotes the emission metric value from a single model m for species i, region r, and season s. $M_{\mathrm{max}}(i)$ is the maximum GTP(20) value found in any region (Europe, East Asia, and global) and season (NH summer and winter) for species i, while $M_{\mathrm{min}}(i)$ is the minimum value.

The values of NV_{BE} are numbers between 0 and 1. As GTP(20) values from individual models can be larger than the maximum from the best estimate and smaller than the minimum, $NV_m(r,s,i)$ can be larger than 1 or negative, respectively. Figure 4 is a scatter plot between NV_{BE} and all the individual NV_m values, where the colors indicate model and shapes of the symbol indicate component. Since the processes that could lead to correlations are somewhat different for aerosols and ozone precursors (e.g., non-linear chemistry effects for the latter) the species are split into two separate panels.

Figure 4 clearly shows the correlation between the species for the individual model emission metrics. For the aerosols, HadGEM and NorESM tend to give higher (in absolute terms, i.e., more negative for cooling agents) emission metric values compared to the best estimate, while ECHAM gives much lower values. For the ozone precursors, the picture is the opposite, with NorESM being lower than the BE while the OsloCTM is higher. This indicates that for both aerosols and ozone precursors there are generic features in the models related to representation of key processes (e.g., vertical mixing, wet scavenging, ozone production efficiency) that systematically affects the emission metric values.

These correlations between the estimates for the individual species have to be taken into account when the uncertainty in the net effect of a multi-component mitigation policy is estimated. Since different SLCFs are often co-emitted, most mitigation options will affect emissions of several species at the same time. The uncertainty in the estimate of the net effect depends on the composition of the mitigation, i.e., mix of species, regions, and sectors. To be useful for policymaking, the emission metrics should be robust enough so that there is trust in the sign of the net effect of a mitigation measure and that the uncertainty in the emission metrics does not hinder a ranking of different measures when cost efficiency is considered. Figure 5 shows the estimates of the net effect (here in terms of temperature change after 20 years, i.e., using AGTP(20) for pulse emissions) when using the sets of emission metrics from the individual models. First, we consider a global mitigation of a 10 % reduction in emissions of all SLCFs for which the best estimate is positive for the AGTP(20) (BC, OC, and VOCs – labeled B in Fig. 5),

and then a 10 % global reduction in all SLCFs (an extreme case of also reducing the co-emitted cooling species OC, SO_2, and NO_x – case A in Fig. 5). The shipping sector is not included in this sensitivity test as the best estimate is only based on two models. ECHAM6 did not calculate RFs for the ozone precursors; therefore, values for the best estimate are given for those species. NH_3 is not included, as only OsloCTM2 provided RF estimates of that. These scenario estimates are based on emission inventories for 2008 (Klimont et al., 2016). For a 10 % reduction in emissions of the warming SLCFs (BC, CO, and VOCs), the best estimate gives a global reduction in temperature of 0.61 mK 20 years after a pulse, with a spread of −0.38 to −0.85 mK. When the cooling components are included, the best estimate gives a global warming of 0.49 mK, with models ranging from 0.06 to 0.49 mK. Hence, all models agree that a reduction in those six SLCFs will cause warming, but for one of the models there is only a marginal warming.

The black bars in Fig. 5 give the uncertainty in the net global temperature effect assuming all the metric values are independent. This gives a similar or narrower uncertainty interval than the spread of the estimates using the individual model metrics, again showing that there is considerable correlation in the model estimates. However, if the difference between the models were 100 % systematic (i.e., one model always giving the lowest estimates by magnitude and another model giving the highest), then the model-based interval would be given by the blue bar in Fig. 5. From this analysis, we conclude that the uncertainty for an estimate of the net temperature effect of multi-component emission change is enhanced due to the correlations; however, for mitigation measures that mainly change emissions of species with positive GTPs, the sign of the global temperature signal is robust.

Since not all processes are included in all the models, the average of all models in Fig. 5 will differ from the best estimate. This deviation is observed in both scenarios but is clearest for a mitigation scenario including both warming and cooling SLCFs, as the net climate impact is a sum of large positive and negative numbers. The processes not included are dominated by cooling. Three out of four models do not include the cooling from the semi-direct effect of BC, nor do they include what is mainly cooling from nitrate for the ozone precursors and SO_2. As a consequence, the individual models tend towards more cooling or less warming than the best estimate for a mitigation scenario of SLCFs.

Our findings show that the robustness is largest for individual species, i.e., what region and season of emissions to mitigate for an individual species. Next follows a subgroup of species that correlates, such as aerosols. Lowest robustness is given for mitigation for all SLCFs. However, we observe that all models agree whether two hypothetical mitigation scenarios give warming or cooling.

3.1.5 Variations with time horizon

We have until now presented emission metric values at certain fixed time horizons; however, these values vary greatly with time horizon, which is partially controlled by CO_2. SLCFs impact the atmosphere for a short time, as aerosols and aerosol precursors have atmospheric lifetimes of about a week. Methane, however, has an atmospheric perturbation lifetime of about 12.4 years (IPCC, 2013). Due to the inertia in the climate system, the climate is impacted for at least 10–20 years from a radiative forcing lasting only a week (Peters et al., 2011; Solomon et al., 2010; Fuglestvedt et al., 2010). The denominator in the emission metrics is CO_2, which impacts the atmosphere for centuries (IPCC, 2013). However, aerosols are very strong at perturbing the radiative balance of the Earth while they are situated in the atmosphere; for instance, the radiative efficiency ($Wm^{-2}\,kg^{-1}$) of black carbon is about a million times larger than the radiative efficiency of CO_2. Thus, the magnitude of the normalized emission metric values is very high for short time horizons but decreases rapidly with increasing time horizon. The aerosols have the highest emission metric values in magnitude for the shortest time horizons, see Figs. 6 and 7 for GTP and GWP values in the first 50 years after a pulse emission. Additional figures are provided in the Supplement. NO_x often has a positive emission metric value for the first 5–10 years, followed by negative numbers, as the sum of the short-lived effects are positive and the longer-lived effect negative. However (see Fig. 7), we find cooling already from year one for emissions in Europe during all seasons and East Asia during winter as the cooling from the aerosol effect is as large as or larger than the short-lived ozone effect. This aerosol effect is cooling for all regions, while the models disagree about the impact for shipping. The results for the shipping sector should be considered with care as the best estimate is based on only two models with large inter-model variability. The time dimension is especially important for NO_x and the other ozone precursors, as different regions and seasons are given different weights with different time horizons. For instance, shipping in summer has most positive GTP values for NO_x of all cases in the first 10 years but becomes the second most negative after 20 years. For a specific region and season, the weighting between the aerosols and ozone precursors is also changing with variable time horizon.

3.2 Global temperature response

We have applied the emission metrics on an emission dataset for year 2008 (Klimont et al., 2016). The variability discussed in the previous section is also found in the global temperature response for regional and seasonal emissions (Fig. 8). A seasonal profile is included in the emissions, with typically largest emissions in the winter season, but the temperatures should be taken as being annual mean values. The temperature response drops rapidly off due to the short life-

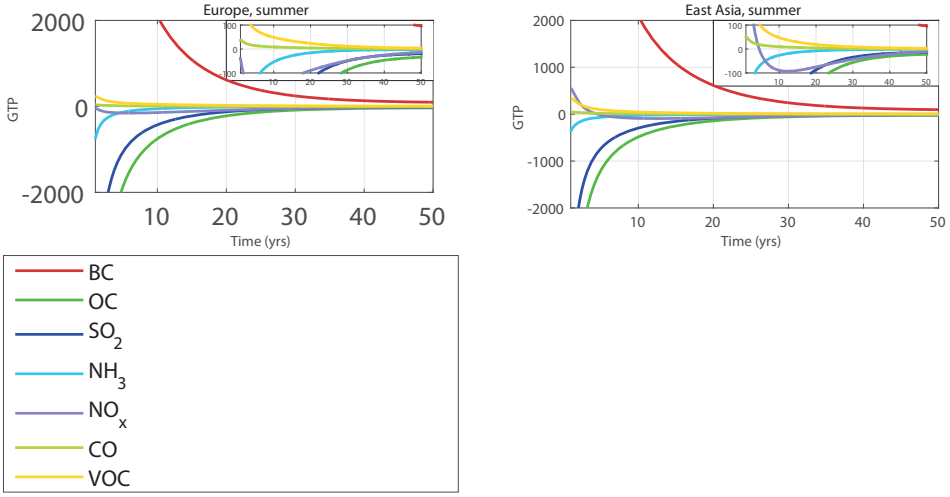

Figure 6. A comparison of GTP values, as a function of time horizon, for summer emissions in Europe (left) and East Asia (right).

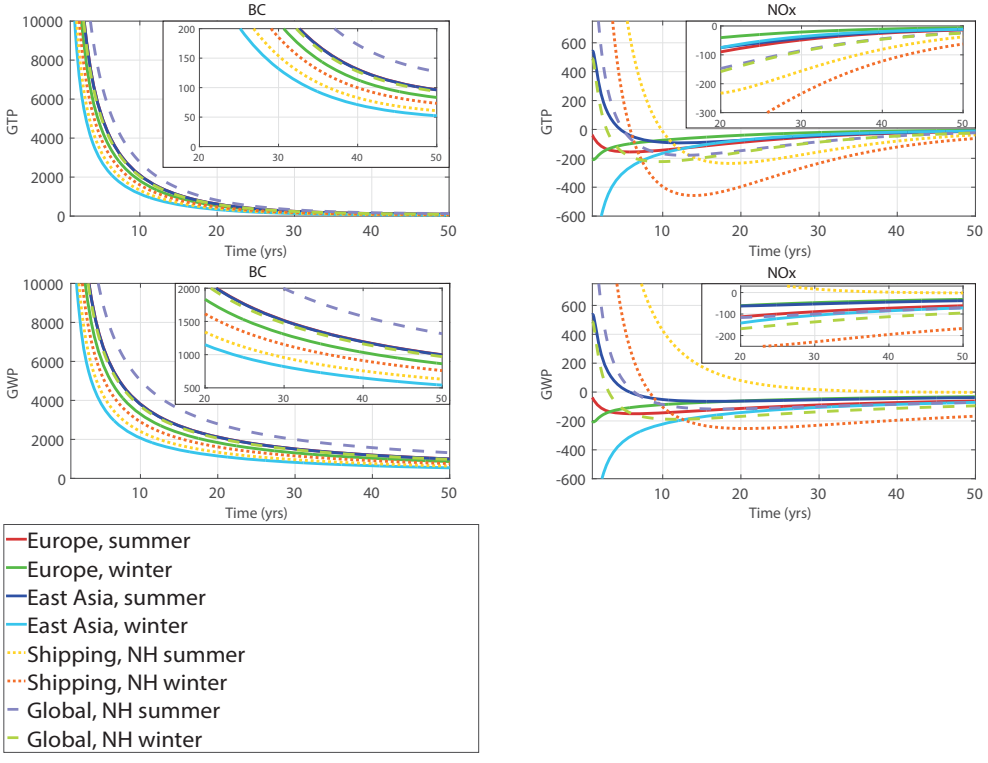

Figure 7. GTPs (top) and GWPs (bottom) for BC (left) and NO_x (right) as a function of time horizon, for all emission cases.

times of the SLCFs. The response of the SO_2 emissions appears to decay more slowly than for the NO_x emissions between 50 and 100 years, which might not be expected given that the SO_2 response has only a short-lived component. This apparently peculiar behavior occurs since the net response of NO_x emissions is a sum of partially canceling warming and cooling processes, and the degree of cancellation varies with time. The processes related to CH_4 have a longer response tail than the aerosol-related processes. In general, the total temperature response is governed by the SO_2 emissions. Hence, the total climate impact is a cooling for all regions and seasons but is largest for emissions in summer. The emission mix is different between the regions. For instance, SO_2 and NO_x generally dominate for shipping. Europe and East Asia have a broader mix of SLCFs that impact the climate. The temperature perturbation, dominated by cooling, is in

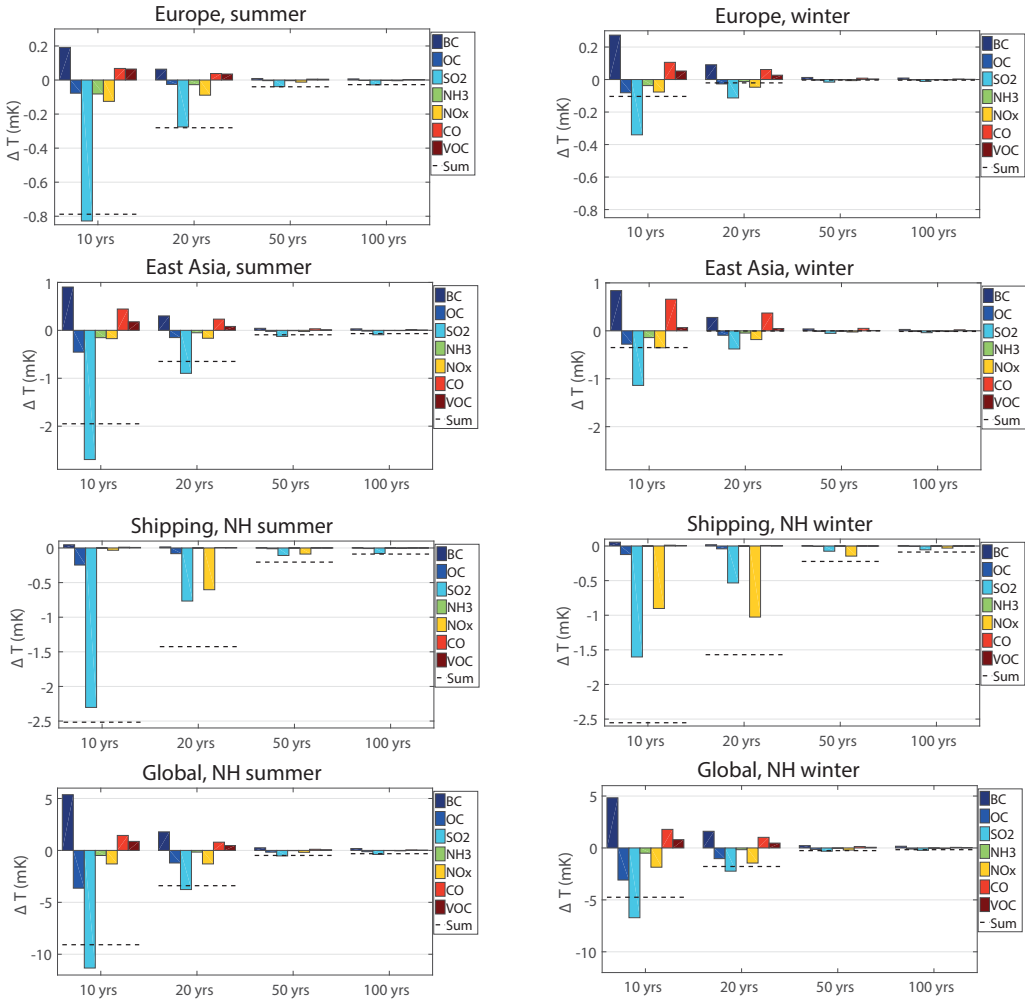

Figure 8. The global temperature response 10, 20, 50, and 100 years after regional and seasonal emissions in 2008. The regions from top to bottom are Europe, East Asia, the global shipping sector, and global. NH summer season (May–October) is to the left and NH winter season (November–April) to the right. Note that the y axis differs between the regions.

agreement with Aamaas et al. (2013), who also showed that the warming from global emissions of CO_2 is larger than the net cooling from the SLCFs after only 15 years. We have presented the global temperature response, while regional variations will occur beyond this global mean response (e.g., Lund et al., 2012).

3.3 Gradual implementation of mitigation

We have calculated emission metrics for pulse emissions, which is the standard method. However, changes in emissions are often gradual in real life. In this section, we present how the emission metric values differ based on a gradual implementation of mitigation policy (see Fig. 9), which is calculated by convolution as given in Eq. (6). We show results only for a ramping period of 15 years, but we have also looked at other implementation rates. The emission metric values presented here are for Europe in the summer season, with the exception of CH_4, for which, for illustrative reasons, the parameterizations in Myhre et al. (2013) are applied.

For species that have a shorter influence on the climate system than CO_2, the normalized emission metric values will almost always be larger in magnitude for sustained emissions than pulse emissions. The only exception is for species with counteracting processes on different timescales, such as for NO_x in Fig. 9. The 15-year ramping scenarios give slightly higher normalized emission metrics than the sustained case (again with the exception of NO_x at short time horizons), but those emission metric values approach each other in the long term. The longer the ramping period lasts, the larger the emission metric value becomes, but the value converges to the sustained emission case for time horizons beyond the ramping period. The normalized emission metric values are higher in the ramping scenarios than the sustained case since the impact of the shorter-lived effects are given more weight than CO_2 which is undergoing the same ramping scenario.

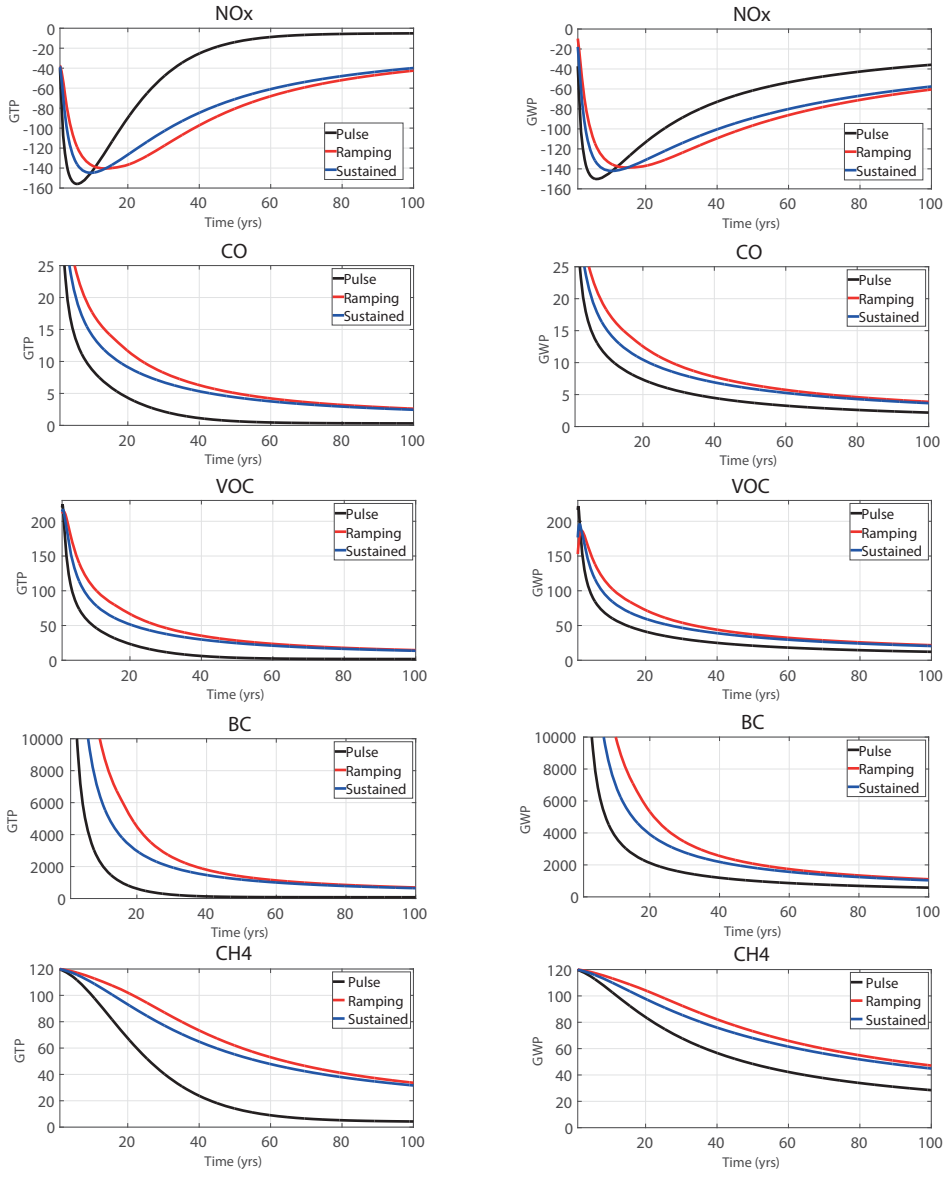

Figure 9. The emission metric values for different types of emission profiles for European emissions in summer, with GTP to the left and GWP to the right. The ramping period is set to 15 years. We include NO_x, CO, and VOCs (top) as ozone precursors that include processes that alter the atmospheric chemistry on both monthly and yearly scales and BC (middle) representing particle emissions with an atmospheric lifetime of about a week. To put this into perspective, we also show CH_4 (bottom), which perturbs the atmosphere with a lifetime of roughly 12 years.

Hence, a mitigation scenario that will have a gradually increasing effect over several years will, for most species, have a higher metric value than for mitigation that instantly takes effect. What this means is that one obtains the benefit of mitigating SLCFs (i.e., higher CO_2 equivalent emission reduction and thus higher value on an emission trading market or in a cost-effectiveness analysis) as soon as those reductions begin. The reason is the planned emission reductions of the shorter-lived species close to the time horizon has a large impact. Hence, these emission metrics for ramping scenarios should be used with care. If there is a chance that the emission reductions are reversible and will not be kept in place (or replaced by even stronger reductions) until the time horizon, the ramping metrics will overestimate the effects.

We also present the temporal evolution for all the regions and seasons for BC and NO_x in Fig. 10, while Fig. 9 only showed these emission metric values for Europe in summer. While the regions and seasons are ranked the same for all time horizons for the aerosols, the ranking may differ for the ozone precursors for different emission metrics and different time horizons due to competing processes on different timescales, especially for NO_x.

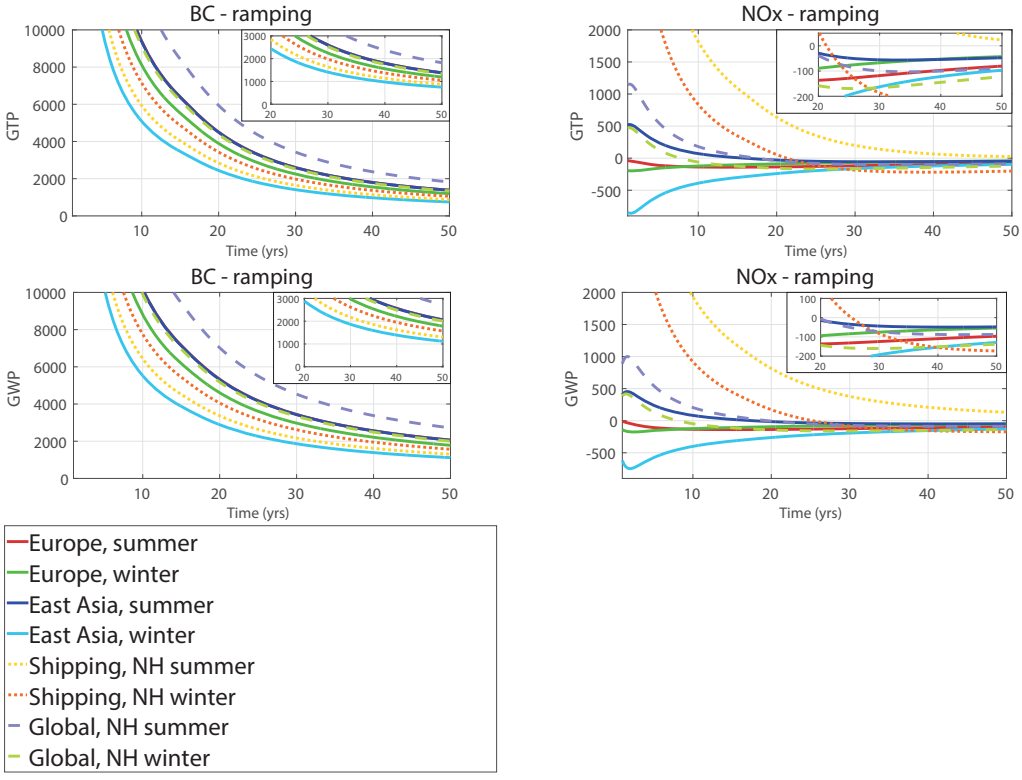

Figure 10. The emission metric values for ramping scenario emissions. GTP (top) and GWP (bottom) are given for BC (left) and NO_x (right).

The other significant difference between emission metrics based on pulse and ramping emissions is the sign switch for NO_x (see Fig. 7). In the pulse case, the GTP values are negative or turn negative within the first 6 years for all cases except summer shipping when sign switch takes 10 years. The sign switch is much slower for the ramping scenario emission metrics. Even after 10 years, half of the cases give positive GTP values (see Fig. 10). In the long run (> 22 years), all the GTP values with the exception of shipping in summer, are negative. Thus, if a time horizon of 10 years is picked, the mitigation policies of NO_x will depend highly on the assumed emission scenario.

3.4 Policy implications

Emission metrics can be applied as an "exchange rate" between different emissions in climate polices, such as for different LLGHGs in the Kyoto Protocol. While the calculations of how emissions impact the climate build on scientific knowledge, how the emission metrics should be used is given by political choices. There is no particular reason why there should be one and only one goal for our climate policy (Fuglestvedt et al., 2000; Rypdal et al., 2005; Daniel et al., 2012; Sarofim, 2012; Jackson, 2009; Victor and Kennel, 2014). In particular there may be harmful impacts of exceeding a long-term temperature constraint (e.g., 2 °C), while at the same time there is more immediate concern about short term effects over the next decade or so. The rationale behind a climate policy focusing on SLCFs must be that there are potential harmful effects of climate change over the next few decades. However, CO_2 and other LLGHGs should also be included in evaluation of possible mitigation measures under a short-term goal as these species also influence the climate on short timescales. Historically, emission metrics within international climate policy have been applied to emissions of LLGHGs. However, as the uncertainty for the emission metrics of SLCFs is reduced and the values become more robust, this opens up for regimes that also include non-methane SLCFs beyond CH_4, e.g., CCAC. Recently, Mexico included BC in their intended nationally determined contribution (INDC) submitted to the UNFCCC (Mexico, 2015). But, as pointed out by Allen et al. (2016), a generic "CO_2-equivalent" emission reduction target by a given year, defined in terms of GWP(100) and containing a substantial element of SLCF mitigation, represents an ambiguous commitment to future climate.

A general difference between LLGHGs and SLCFs is that the location of the LLGHG emissions does not matter, while we have shown that different locations, as well as timing of emissions, will cause different impacts of SLCFs (Fuglestvedt et al., 1999; Naik et al., 2005; Berntsen et al., 2006; Shindell and Faluvegi, 2009; Berntsen et al., 2005). In ad-

dition to differences in the total global response, the spatial distribution of the impact depends on the location and timing of the SLCFs emissions. Further, we have shown that individual models may give significantly different emission metric values than other models.

4 Conclusions

We have presented emission metrics for regional emissions of several SLCFs (BC, OC, SO_2, NH_3, NO_x, CO, and VOCs) based on four different models. We have focused on the emission regions Europe and East Asia but have also given numbers for the global shipping sector and total emissions from all countries. Values have been estimated for emissions in both the summer and winter seasons. For the aerosols, the magnitude of the emission metric values is larger for Europe than East Asia and for summer than winter. The variability between the models is generally larger than the variations between regions and seasons. However, most models agree that specific regions and seasons have larger emission metric values than others. Hence, the robustness of this ranking is better than can be interpreted from the variability between models. The co-variability between models is also seen for the ozone precursors. For CO, the emission metric values are larger for East Asia than Europe and for winter than summer. The pattern is the opposite for VOCs with larger emission metric values in Europe and in summer. NO_x is more complex with more negative values in summer than winter for Europe. In East Asia, we model no significant difference between the seasons for GTP(20) for NO_x, while the GWP(100) for winter emissions is more negative.

We have also calculated emission metrics for transient scenarios where we consider a ramping of the emission over time. This emission metric will better represent the effect of imposing a mitigation measure (i.e., a new technology standard) that is known to give a long-term change in emissions. For species that have a shorter influence on the atmosphere than CO_2, the magnitude of the emission metric value is larger for a mitigation scenario with a gradually increasing effect over several years than for the standard pulse-based emission metric. The only exception is species that have competing short- and longer-lived effects that are positive and negative, notably for NO_x.

We observe variability in the emission metrics between different regions and seasons, but with varying robustness between the models. As the certainties in the numbers increases, the regional and seasonal differences may be accounted for in mitigation policies, agreements, and potential trading schemes involving SLCFs. One robust finding in our study is that, per unit mass of emissions, emissions of aerosols and their precursors in Europe should likely be given more weight than emissions in East Asia, as well as emissions in summer likely more weight than in winter. When emission metrics are applied, the selection of the specific emission metric and time horizon is of significance. The emission metric values for SLCFs drop quickly with time horizon. For the ozone precursors, the ranking between different regions and seasons can vary with different time horizon. Thus, emission metrics must be used based on careful consideration of these factors.

5 Data availability

The RF data applied are given by Bellouin et al. (2016).

The Supplement related to this article is available online at doi:10.5194/acp-16-7451-2016-supplement.

Acknowledgements. The authors would like to acknowledge the support from the European Union Seventh Framework Programme (FP7/2007-2013) under grant agreement no. 282688 – ECLIPSE, as well as funding by the Norwegian Research Council within the projects "Climate and health impacts of Short-Lived Atmospheric Components (SLAC)" and "the Role of Short-Lived Climate Forcers in the Global Climate Regime" (project no. 235548). We thank Øivind Hodnebrog and Dirk Olivié for providing radiative forcing data and Glen Peters for comments. We thank the two anonymous referees and the editor for valuable comments that improved the paper.

Edited by: K. Tsigaridis

References

Aamaas, B., Peters, G. P., and Fuglestvedt, J. S.: Simple emission metrics for climate impacts, Earth Syst. Dynam., 4, 145–170, doi:10.5194/esd-4-145-2013, 2013.

Allen, M. R., Fuglestvedt, J. S., Shine, K. P., Reisinger, A., Pierrehumbert, R. T., and Forster, P. M.: New use of global warming potentials to compare cumulative and short-lived climate pollutants, Nature Clim. Change, doi:10.1038/nclimate2998, 2016.

Bellouin, N., Rae, J., Jones, A., Johnson, C., Haywood, J., and Boucher, O.: Aerosol forcing in the Climate Model Intercomparison Project (CMIP5) simulations by HadGEM2-ES and the role of ammonium nitrate, J. Geophys. Res.-Atmos., 116, D20206, doi:10.1029/2011JD016074, 2011.

Bellouin, N., Baker, L., Hodnebrog, Ø., Olivié, D., Cherian, R., Macintosh, C., Samset, B., Esteve, A., Aamaas, B., Quaas, J., and Myhre, G.: Regional and seasonal radiative forcing by perturbations to aerosol and ozone precursor emissions, Atmos. Chem. Phys. Discuss., doi:10.5194/acp-2016-310, in review, 2016.

Bentsen, M., Bethke, I., Debernard, J. B., Iversen, T., Kirkevåg, A., Seland, Ø., Drange, H., Roelandt, C., Seierstad, I. A., Hoose, C., and Kristjánsson, J. E.: The Norwegian Earth System Model, NorESM1-M – Part 1: Description and basic evaluation of the physical climate, Geosci. Model Dev., 6, 687–720, doi:10.5194/gmd-6-687-2013, 2013.

Berntsen, T., Fuglestvedt, J. S., Joshi, M., Shine, K., Stuber, N., Li, L., Hauglustaine, D., and Ponater, M.: Climate response to regional emissions of ozone precursers: sensitivities and warming potentials, Tellus B, 57, 283–304, 2005.

Berntsen, T., Fuglestvedt, J. S., Myhre, G., Stordal, F., and Berglen, T. F.: Abatement of greenhouse gases: Does location matter?, Climatic Change, 74, 377–411, 2006.

Boer, G. B. and Yu, B. Y.: Climate sensitivity and response, Clim. Dynam., 20, 415–429, doi:10.1007/s00382-002-0283-3, 2003.

Bond, T. C., Zarzycki, C., Flanner, M. G., and Koch, D. M.: Quantifying immediate radiative forcing by black carbon and organic matter with the Specific Forcing Pulse, Atmos. Chem. Phys., 11, 1505–1525, 10.5194/acp-11-1505-2011, 2011.

Bond, T. C., Doherty, S. J., Fahey, D. W., Forster, P. M., Berntsen, T., DeAngelo, B. J., Flanner, M. G., Ghan, S., Kärcher, B., Koch, D., Kinne, S., Kondo, Y., Quinn, P. K., Sarofim, M. C., Schultz, M. G., Schulz, M., Venkataraman, C., Zhang, H., Zhang, S., Bellouin, N., Guttikunda, S. K., Hopke, P. K., Jacobson, M. Z., Kaiser, J. W., Klimont, Z., Lohmann, U., Schwarz, J. P., Shindell, D., Storelvmo, T., Warren, S. G., and Zender, C. S.: Bounding the role of black carbon in the climate system: A scientific assessment, J. Geophys. Res.-Atmos., 118, 5380–5552, 10.1002/jgrd.50171, 2013.

Boucher, O. and Reddy, M. S.: Climate trade-off between black carbon and carbon dioxide emissions, Energ. Policy, 36, 193–200, 2008.

Bowerman, N. H. A., Frame, D. J., Huntingford, C., Lowe, J. A., Smith, S. M., and Allen, M. R.: The role of short-lived climate pollutants in meeting temperature goals, Nature Clim. Change, 3, 1021–1024, doi:10.1038/nclimate2034, 2013.

Bridgeman, C. H., Pyle, J. A., and Shallcross, D. E.: A three-dimensional model calculation of the ozone depletion potential of 1-bromopropane (1-C3H7Br), J. Geophys. Res.-Atmos., 105, 26493–26502, doi:10.1029/2000JD900293, 2000.

Collins, W. J., Sitch, S., and Boucher, O.: How vegetation impacts affect climate metrics for ozone precursors, J. Geophys. Res., 115, D23308, doi:10.1029/2010jd014187, 2010.

Collins, W. J., Fry, M. M., Yu, H., Fuglestvedt, J. S., Shindell, D. T., and West, J. J.: Global and regional temperature-change potentials for near-term climate forcers, Atmos. Chem. Phys., 13, 2471–2485, doi:10.5194/acp-13-2471-2013, 2013.

Daniel, J., Solomon, S., Sanford, T., McFarland, M., Fuglestvedt, J., and Friedlingstein, P.: Limitations of single-basket trading: lessons from the Montreal Protocol for climate policy, Climatic Change, 111, 241–248, doi:10.1007/s10584-011-0136-3, 2012.

Fry, M. M., Naik, V., West, J. J., Schwarzkopf, D., Fiore, A., Collins, W. J., Dentener, F., Shindell, D. T., Atherton, C. S., Bergmann, D. J., Duncan, B. N., Hess, P. G., MacKenzie, I. A., Marmer, E., Schultz, M. G., Szopa, S., Wild, O., and Zeng, G.: The influence of ozone precursor emissions from four world regions on tropospheric composition and radiative climate forcing, J. Geophys. Res., 117, D07306, doi:10.1029/2011JD017134, 2012.

Fuglestvedt, J. S., Berntsen, T. K., Isaksen, I. S. A., Mao, H., Liang, X.-Z., and Wang, W.-C.: Climatic forcing of nitrogen oxides through changes in tropospheric ozone and methane; global 3D model studies, Atmos. Environ., 33, 961–977, doi:10.1016/s1352-2310(98)00217-9, 1999.

Fuglestvedt, J. S., Berntsen, T., Godal, O., and Skovdin, T.: Climate implications of GWP-based reductions in greenhouse gas emissions, Geophys. Res. Lett., 27, 409–412, 2000.

Fuglestvedt, J. S., Berntsen, T. K., Godal, O., Sausen, R., Shine, K. P., and Skodvin, T.: Metrics of climate change: Assessing radiative forcing and emission indices, Climatic Change, 58, 267–331, 2003.

Fuglestvedt, J. S., Shine, K. P., Berntsen, T., Cook, J., Lee, D. S., Stenke, A., Skeie, R. B., Velders, G. J. M., and Waitz, I. A.: Transport impacts on atmosphere and climate: Metrics, Atmos. Environ., 44, 4648–4677, 2010.

Hewitt, H. T., Copsey, D., Culverwell, I. D., Harris, C. M., Hill, R. S. R., Keen, A. B., McLaren, A. J., and Hunke, E. C.: Design and implementation of the infrastructure of HadGEM3: the next-generation Met Office climate modelling system, Geosci. Model Dev., 4, 223–253, doi:10.5194/gmd-4-223-2011, 2011.

Hodnebrog, Ø., Myhre, G., and Samset, B. H.: How shorter black carbon lifetime alters its climate effect, Nat. Commun., 5, 5065, doi:10.1038/ncomms6065, 2014.

Holmes, C. D., Tang, Q., and Prather, M. J.: Uncertainties in climate assessment for the case of aviation NO, Proc. Natl. Acad. Sci. USA, 108, 10997–11002, doi:10.1073/pnas.1101458108, 2011.

Holmes, C. D., Prather, M. J., and Vinken, G. C. M.: The climate impact of ship NO_x emissions: an improved estimate accounting for plume chemistry, Atmos. Chem. Phys., 14, 6801–6812, doi:10.5194/acp-14-6801-2014, 2014.

IPCC: Climate Change: The IPCC Scientific Assessment, edited by: Houghton, J. T., Jenkins, G. J., and Ephraums, J. J., Cambridge University Press, Cambridge, United Kingdom, 1990.

IPCC: The Physical Science Basis. Contribution of Working Group I to the Fifth Assessment Report of the Intergovernmental Panel on Climate Change, edited by: Stocker, T. F., Qin, D., Plattner, G. K., Tignor, M., Allen, S. K., Boschung, J., Nauels, A., Xia, Y., Bex, V., and Midgley, P. M., Cambridge University Press, Cambridge, United Kingdom and New York, NY, USA, 1535 pp., 2013.

Iversen, T., Bentsen, M., Bethke, I., Debernard, J. B., Kirkevåg, A., Seland, Ø., Drange, H., Kristjansson, J. E., Medhaug, I., Sand, M., and Seierstad, I. A.: The Norwegian Earth System Model, NorESM1-M – Part 2: Climate response and scenario projections, Geosci. Model Dev., 6, 389–415, doi:10.5194/gmd-6-389-2013, 2013.

Jackson, S. C.: Parallel Pursuit of Near-Term and Long-Term Climate Mitigation, Science, 326, 526–527, doi:10.1126/science.1177042, 2009.

Joos, F., Roth, R., Fuglestvedt, J. S., Peters, G. P., Enting, I. G., von Bloh, W., Brovkin, V., Burke, E. J., Eby, M., Edwards, N. R., Friedrich, T., Frölicher, T. L., Halloran, P. R., Holden, P. B., Jones, C., Kleinen, T., Mackenzie, F. T., Matsumoto, K., Meinshausen, M., Plattner, G.-K., Reisinger, A., Segschneider, J., Shaffer, G., Steinacher, M., Strassmann, K., Tanaka, K., Timmermann, A., and Weaver, A. J.: Carbon dioxide and climate impulse response functions for the computation of greenhouse gas metrics: a multi-model analysis, Atmos. Chem. Phys., 13, 2793–2825, doi:10.5194/acp-13-2793-2013, 2013.

Klimont, Z., Höglund-Isaksson, L., Heyes, C., Rafaj, P., Schöpp, W., Cofala, J., Purohit, P., Borken-Kleefeld, J., Kupiainen, K., Kiesewetter, G., Winiwarter, W., Amann, M., Zhao, B., Wang, S.

X., Bertok, I., and Sander, R.: Global scenarios of air pollutants and methane: 1990–2050, in preparation, 2016.

Lund, M., Berntsen, T., Fuglestvedt, J., Ponater, M., and Shine, K.: How much information is lost by using global-mean climate metrics? an example using the transport sector, Climatic Change, 113, 949–963, doi:10.1007/s10584-011-0391-3, 2012.

Mexico: Intended Nationally Determined Contribution: available at: http://www4.unfccc.int/submissions/INDC/Published20Documents/Mexico/1/MEXICO20INDC2003.30.2015.pdf, last access: 30 June 2015.

Myhre, G., Berglen, T. F., Johnsrud, M., Hoyle, C. R., Berntsen, T. K., Christopher, S. A., Fahey, D. W., Isaksen, I. S. A., Jones, T. A., Kahn, R. A., Loeb, N., Quinn, P., Remer, L., Schwarz, J. P., and Yttri, K. E.: Modelled radiative forcing of the direct aerosol effect with multi-observation evaluation, Atmos. Chem. Phys., 9, 1365–1392, doi:10.5194/acp-9-1365-2009, 2009.

Myhre, G., Fuglestvedt, J. S., Berntsen, T. K., and Lund, M. T.: Mitigation of short-lived heating components may lead to unwanted long-term consequences, Atmos. Environ., 45, 6103–6106, doi:10.1016/j.atmosenv.2011.08.009, 2011.

Myhre, G., Shindell, D., Bréon, F.-M., Collins, B., Fuglestvedt, J. S., Huang, J., Koch, D., Lamarque, J.-F., Lee, D., Mendoza, B., Nakajima, T., Robock, A., Stephens, G., Takemura, T., and Zhang, H.: Anthropogenic and Natural Radiative Forcing, in: Climate Change 2013: The Physical Science Basis. Contribution of Working Group I to the Fifth Assessment Report of the Intergovernmental Panel on Climate Change, edited by: Stocker, T. F., Qin, D., Plattner, G. K., Tignor, M., Allen, S. K., Boschung, J., Nauels, A., Xia, Y., Bex, V., and Midgley, P. M., Cambridge University Press, Cambridge, United Kingdom and New York, NY, USA, 2013.

Naik, V., Mauzerall, D., Horowitz, L., Schwarzkopf, M. D., Ramaswamy, V., and Oppenheimer, M.: Net radiative forcing due to changes in regional emissions of tropospheric ozone precursors, J. Geophys. Res., 110, D24306, 10.1029/2005jd005908, 2005.

Olivié, D. J. L. and Peters, G. P.: Variation in emission metrics due to variation in CO_2 and temperature impulse response functions, Earth Syst. Dynam., 4, 267–286, doi:10.5194/esd-4-267-2013, 2013.

Olsen, S. C., Hannegan, B. J., Zhu, X., and Prather, M. J.: Evaluating ozone depletion from very short-lived halocarbons, Geophys. Res. Lett., 27, 1475–1478, doi:10.1029/1999GL011040, 2000.

Paoli, R., Cariolle, D., and Sausen, R.: Review of effective emissions modeling and computation, Geosci. Model Dev., 4, 643–667, doi:10.5194/gmd-4-643-2011, 2011.

Peters, G., Aamaas, B., Berntsen, T., and Fuglestvedt, F. S.: The integrated Global Temperature Change Potential (iGTP) and relationship with other simple emission metrics, Environ. Res. Lett., 6, 044021, doi:10.1088/1748-9326/6/4/044021, 2011.

Pierrehumbert, R.: Short-Lived Climate Pollution, Ann. Rev. Earth Planet. Sci., 42, 341–379, doi:10.1146/annurev-earth-060313-054843, 2014.

Prather, M. J.: Lifetimes of atmospheric species: Integrating environmental impacts, Geophys. Res. Lett., 29, 20-21–20-23, doi:10.1029/2002GL016299, 2002.

Rogelj, J., Schaeffer, M., Meinshausen, M., Shindell, D. T., Hare, W., Klimont, Z., Velders, G. J. M., Amann, M., and Schellnhuber, H. J.: Disentangling the effects of CO_2 and short-lived climate forcer mitigation, Proc. Natl. Acad. Sci., 111, 16325–16330, doi:10.1073/pnas.1415631111, 2014.

Rypdal, K., Berntsen, T., Fuglestvedt, J. S., Aunan, K., Torvanger, A., Stordal, F., Pacyna, J. M., and Nygaard, L. P.: Tropospheric ozone and aerosols in climate agreements: scientific and political challenges, Environ. Sci. Policy, 8, 29–43, doi:10.1016/j.envsci.2004.09.003, 2005.

Sarofim, M.: The GTP of Methane: Modeling Analysis of Temperature Impacts of Methane and Carbon Dioxide Reductions, Environ. Model. Assess., 17, 231–239, doi:10.1007/s10666-011-9287-x, 2012.

Schmale, J., Shindell, D., von Schneidemesser, E., Chabay, I., and Lawrence, M.: Clean up our skies, Nature, 515, 335–337, 2014.

Shindell, D. and Faluvegi, G.: Climate response to regional radiative forcing during the twentieth century, Nat. Geosci., 2, 294–300, 2009.

Shindell, D., Schulz, M., Ming, Y., Takemura, T., Faluvegi, G., and Ramaswamy, V.: Spatial scales of climate response to inhomogeneous radiative forcing, J. Geophys. Res.-Atmos., 115, D19110, doi:10.1029/2010JD014108, 2010.

Shindell, D. T., Faluvegi, G., Koch, D. M., Schmidt, G. A., Unger, N., and Bauer, S. E.: Improved Attribution of Climate Forcing to Emissions, Science, 326, 716–718, doi:10.1126/science.1174760, 2009.

Shine, K. P., Fuglestvedt, J. S., Hailemariam, K., and Stuber, N.: Alternatives to the Global Warming Potential for Comparing Climate Impacts of Emissions of Greenhouse Gases, Climatic Change, 68, 281–302, doi:10.1007/s10584-005-1146-9, 2005.

Shine, K. P., Berntsen, T., Fuglestvedt, J. S., Stuber, N., and Skeie, R. B.: Comparing the climate effect of emissions of short and long lived climate agents, Philos. Trans. Roy. Soc. A, 365, 1903–1914, 2007.

Shoemaker, J. K., Schrag, D. P., Molina, M. J., and Ramanathan, V.: What Role for Short-Lived Climate Pollutants in Mitigation Policy?, Science, 342, 1323–1324, doi:10.1126/science.1240162, 2013.

Smith, S. J. and Mizrahi, A.: Near-term climate mitigation by short-lived forcers, Proc. Natl. Acad. Sci., 110, 14202–14206, doi:10.1073/pnas.1308470110, 2013.

Solomon, S., Daniel, J. S., Sanford, T. J., Murphy, D. M., Plattner, G.-K., Knutti, R., and Friedlingstein, P.: Persistence of climate changes due to a range of greenhouse gases, Proc. Natl. Acad. Sci., 107, 18354–18359, doi:10.1073/pnas.1006282107, 2010.

Stevens, B., Giorgetta, M., Esch, M., Mauritsen, T., Crueger, T., Rast, S., Salzmann, M., Schmidt, H., Bader, J., Block, K., Brokopf, R., Fast, I., Kinne, S., Kornblueh, L., Lohmann, U., Pincus, R., Reichler, T., and Roeckner, E.: Atmospheric component of the MPI-M Earth System Model: ECHAM6, J. Adv. Model. Earth Syst., 5, 146–172, doi:10.1002/jame.20015, 2013.

Streets, D. G., Bond, T. C., Carmichael, G. R., Fernandes, S. D., Fu, Q., He, D., Klimont, Z., Nelson, S. M., Tsai, N. Y., Wang, M. Q., Woo, J. H., and Yarber, K. F.: An inventory of gaseous and primary aerosol emissions in Asia in the year 2000, J. Geophys. Res.-Atmos., 108, 8809, doi:10.1029/2002JD003093, 2003.

Søvde, O. A., Gauss, M., Smyshlyaev, S. P., and Isaksen, I. S. A.: Evaluation of the chemical transport model Oslo CTM2 with focus on arctic winter ozone depletion, J. Geophys. Res.-Atmos., 113, D09304, doi:10.1029/2007JD009240, 2008.

Tanaka, K., Peters, G. P., and Fuglestvedt, J. S.: Multi-component climate policy: why do emission metrics matter?, Carbon Management, 1, 191–197, 2010.

Tol, R. S. J., Berntsen, T., O'Neill, B. C., Fuglestvedt, J. S., and Shine, K.: A unifying framework for metrics for aggregating the climate effect of different emissions, Environ. Res. Lett., 7, 044006, doi:10.1088/1748-9326/7/4/044006, 2012.

Victor, D. and Kennel, C. F.: Ditch the 2° C warming goal, Nature, 514, 30–31, doi:10.1038/514030a 2014.

Wild, O., Prather, M. J., and Akimoto, H.: Indirect long-term global radiative cooling from NOx emissions, Geophys. Res. Lett., 28, 1719–1722, 10.1029/2000gl012573, 2001.

Wuebbles, D. J., Patten, K. O., Johnson, M. T., and Kotamarthi, R.: New methodology for Ozone Depletion Potentials of short-lived compounds: n-Propyl bromide as an example, J. Geophys. Res.-Atmos., 106, 14551–14571, doi:10.1029/2001JD900008, 2001.

Yu, H., Chin, M., West, J. J., Atherton, C. S., Bellouin, N., Bergmann, D., Bey, I., Bian, H., Diehl, T., Forberth, G., Hess, P., Schulz, M., Shindell, D., Takemura, T., and Tan, Q.: A multimodel assessment of the influence of regional anthropogenic emission reductions on aerosol direct radiative forcing and the role of intercontinental transport, J. Geophys. Res.-Atmos., 118, 700–720, doi:10.1029/2012JD018148, 2013.